sciendo
ISSN 1335-8871
MEASUREMENT SCIENCE REVIEW
Journal homepage: https://content.sciendo.com

Docking Pose Measurement Method for Large Components Based on Draw-Wire Displacement Sensors

Zheng-yang Sun, Hong-xi Wang*, Hui-hui Tian, Bing Liu

School of Mechatronic Engineering, Xi'an Technological University, 710021, Xi'an, China, wanghongxi@xatu.edu.cn

Abstract: A method for measuring the docking pose of large components based on the draw-wire displacement sensor is proposed. In this method, coordinate systems and measurement points are established on the docking surfaces of fixed and moving components. The draw-wire displacement sensor is used to measure the distances between these measurement points. A mathematical model based on the distances between the measurement points is established, and the three-sphere rendezvous positioning principle is optimized to obtain the spatial positions of the measurement points. Consequently, the pose deviations of the fixed and moving components in all six degrees of freedom (6DOF) are determined. A simulation analysis of the measurement uncertainty of the obtained pose deviations is performed, resulting in a composite standard uncertainty obtained from the measurement standard uncertainties of different sensors. The simulation results show that the composite standard uncertainty is most affected in the *x*-axis translation direction and least affected in the *x*-axis rotation direction. With this method, only the distances between the measurement points need to be measured to determine the corresponding pose relationships. The cost of the equipment is low, and it is not easily affected by external factors such as the environment.

Keywords: Draw-wire displacement sensor, three-sphere rendezvous positioning, spatial pose solution, measurement uncertainty.

1. INTRODUCTION

The assembly and docking of large components is a primary aspect of production and manufacturing. For instance, in aircraft, assembly and docking account for about 50% of the total workload in aircraft production, and the associated costs account for more than 40% of the production cost of an aircraft [1], [2]. With the development of computer technology, automation technology and other industries, manufacturing is moving toward digitization and automation, and digital measurement technology is used in the docking of large components. Digital measurement equipment mainly includes laser trackers, visual measurement systems, etc. However, the docking measurement systems made with this measurement equipment have some drawbacks:

- High manufacturing, transportation and maintenance costs for laser trackers and other devices.
- Susceptible to unstable environmental factors. For instance, laser trackers are susceptible to factors such as temperature, humidity, and air disturbances, especially at transfer stations, and the impact of line-of-sight obstructions and light sources is a major issue during visual measurements [3]-[8].

In order to improve the efficiency of assembly docking and reduce the cost while satisfying the docking accuracy of large component assembly, a method for measuring the docking pose of large components based on a draw-wire displacement sensor is proposed. The using of draw-wire displacement sensors as a digital measurement device is not easily affected by the working environment, is cost-effective and wear-resistant in large component assembly and docking. This is of great significance in expanding the digital assembly and docking method for large components and ensuring the quality of large component assembly.

Currently, there are some applications of draw-wire displacement sensors for spatial pose measurement. Professor Ceccarelli performed an early application of the draw-wire displacement sensor for measuring space pose. Professor Ceccarelli [9] proposed a 3-2-1 configuration of a draw-wire pose measurement mechanism and applied it in areas such as robot workspace evaluation. Zhenjun Luo et al. [10] created a single-line multiplexed three-dimensional measurement system model and proposed the corresponding parameter identification algorithm by combining the characteristics of each measurement system. Jiao Xinquan et al. [11] designed a measurement method and system based on three draw-wire displacement sensors, which better solve the problem of measuring the magnitude of the position change of an object in space. Gang Wang et al. [12] designed a measurement method for a deep-sea pipeline attitude measurement system based on a draw-wire. By using a draw-wire displacement sensor in combination with two magnetically coupled angle sensors and an orthogonal angle sensor, the relative distances

DOI: 10.2478/msr-2023-0027

*Corresponding author: wanghongxi@xatu.edu.cn (H. Wang)

and angles of two subsea pipelines were measured. Bo Zhang et al. [13] used a measurement rope with multiple devices such as two-axis tilt sensors, and based on robot theory and transfer matrix algorithms, developed a measurement model based on different positioning modes to determine the relative position information between the pipes. Current research has used wire displacement sensors in robotic systems or in combination with other sensors to measure the relative poses during docking, but no work has been published on spatial pose determination problem of large component docking surfaces using only wire displacement sensors.

The installation position and connection layout of the draw-wire displacement sensor are very important when performing the pose-resolving calculation, which affects the complexity of the resolving process. As for the pose solution algorithm, in this paper, in conjunction with the relevant researches of previous scholars [14]-[18], the corresponding measurement model is established according to the characteristics of the measurement method, and the analytical calculation process is simplified.

To address the problem of expensive equipment such as laser trackers and machine vision in the assembly inspection of large component docking and the susceptibility to environmental factors such as temperature, humidity, air disturbance, the transfer station and line of sight obstruction leading to misalignment of large component docking, a large component docking position measurement method based on wire displacement sensors is proposed. The corresponding mathematical model is established and solved, and finally the measurement uncertainty of the position deviation obtained by the method is simulated.

2. ESTABLISHMENT OF A POSE MEASUREMENT SYSTEM

Before the two large components are assembled and docked, several sensor mounting points are set up near the docking surfaces of the two components, as shown in Fig. 1 (e.g., the location of the connection flange holes) and several wire sensors are installed between the sensor mounting points of the two components to measure the distance between the two points. The spatial position deviation between the two components is calculated based on the measurement results of the multiple sensors, and the posture of the movable component is adjusted according to the detected deviation during the assembly process (Fig. 1 is only a schematic diagram, the pose adjustment platform can be adjusted in six degrees of freedom).

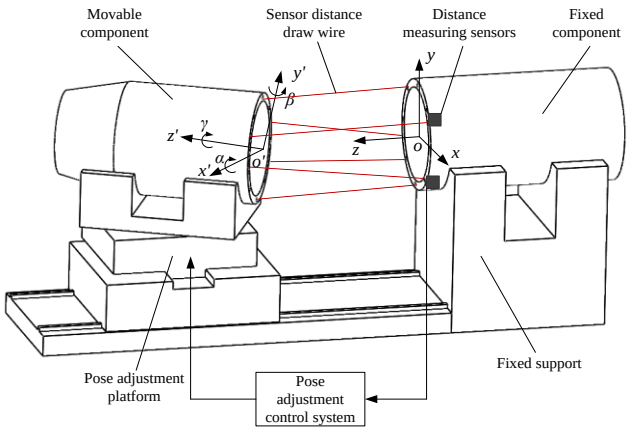

Fig. 1. Schematic diagram of the docking pose measurement method for large components.

For large components for docking pose inspection, the moving component is placed on a platform that can be adjusted for pose. The spatial position of the docking section of the movable component is represented as $o'x'y'z'$, and the spatial position of the docking section of the fixed component is denoted as $oxyz$. Before docking, there are translational position deviations Δx, Δy, angular deviations α, β, γ, and the z-direction is the direction of the docking axis of the two components. The vector (Δx, Δy, Δz) is the position of the origin o′ in the coordinate system {A}. Three non-coincident mounting points are set near the docking surface of the moving component and the fixed component (e.g., at the location of the connection flange hole), and the distance between the corresponding mounting points of the two components is measured using nine draw-wire sensors. The specific adjustment process is shown in the flowchart in Fig. 2.

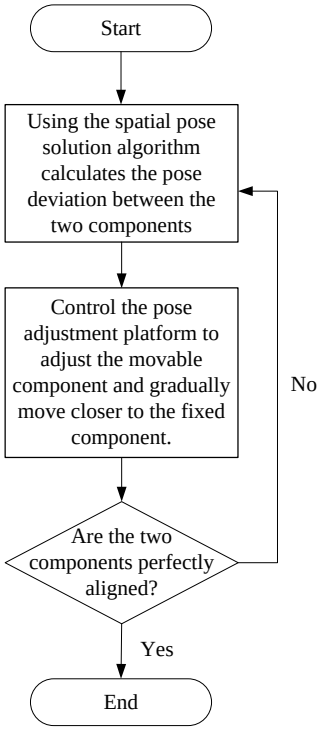

Fig. 2. Flow chart of the adjustment process.

After the adjustment is complete, the pose deviation of the moveable component at this point is zero, i.e.:

$\Delta x = 0$, $\Delta y = 0$, $\alpha = 0$, $\beta = 0$, $\gamma = 0$, $\Delta z = 0$

3. CALCULATION OF RELATIVE SPATIAL POSITIONS

A. Calculation process

The moving coordinate system, the fixed coordinate system, and the installation point are established on the two components. The coordinates of the three points in the fixed coordinate system are known. The coordinates of each point in the moving coordinate system can be derived from the coordinates of the three points in the fixed coordinate system

and the readings from the three draw-wire sensors, and thus the pose of the dynamic coordinate system relative to the fixed coordinate system can be determined. The calculation process for the relative pose of the two components is shown in Fig. 3.

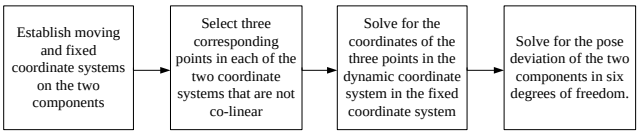

Fig. 3. Relative pose calculation process.

B. Establishment of a mathematical model

As shown in Fig. 4, the lower and upper planes are assumed to be the fixed component docking surface and the moving component docking surface, respectively. The two planes can be fully docked and overlapped. Points A_1, A_2 and A_3 are the measurement reference points on the fixed component docking surface, located at the edge of the fixed component docking surface and correspondingly overlapping with points B_1, B_2 and B_3 on the moving component docking surface. $\Delta A_1A_2A_3$ on the fixed component docking surface is an isosceles right triangle, where A_2A_3 and the midpoint o are the diameter and center of the fixed component docking circle, respectively. Two coordinate systems {A} and {B} are established on the docking surfaces of the fixed component and the moving component, as shown in Fig. 4, with points o and o' as the origins, respectively.

In the model shown in Fig. 4, we assume that the radii of the circular dimensions of the moving and the fixed components are both r. The coordinates of A_1 and A_2 in the coordinate system {A} are $(r, 0, 0)$ and $(0, r, 0)$, respectively, and the coordinates of B_1, B_2 and B_3 in the coordinate system {B} are $(r, 0, 0)$, $(0, r, 0)$, and $(0, -r, 0)$, respectively. The distance between the reference points in the coordinate systems {A} and {B} measured by the draw-wire displacement sensor is r_i, L_{1i}, and L_{2i}, where i = 1, 2, 3.

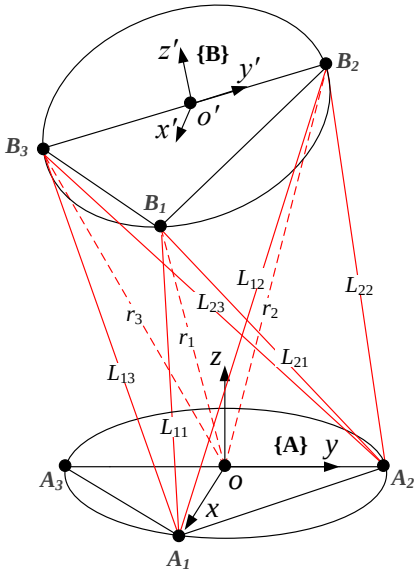

Fig. 4. Selection and connection of measurement points.

C. Calculation of the spatial position of measurement points

Based on the distance between the measured point and the three datum points in space, the unique position coordinates of the measured point can be obtained. The three points on the docking surface of the fixed component can be set as the three datum points. By measuring the distances from these three datum points on the docking surface of the fixed component to the three points on the docking surface of the moving component, the position coordinates of the three points on the docking surface of the moving component in the fixed coordinate system can be determined.

The distance between the three datum points and the measured points on the docking surface of the moving component is measured with three draw-wire displacement sensors. Three spheres with each sensor as the center of the sphere and the measured distance as the radius intersect at two points [19]. The coordinates of the single measured point in the fixed coordinate system are obtained by constraining the initial relative position of the two components. The relative position between the measurement reference point and the point to be measured is shown in Fig. 5. In the fixed coordinate system in which the fixed component is located, the measurement reference points O, A_1 and A_2 correspond to the following three sets of coordinates in sequence:

$$(x_t, y_t, z_t), \quad t = 0,1,2 \tag{1}$$

Assume that the coordinate of the measured point B_i on the docking surface of the moving component in the fixed coordinate system is (x_{Bi}, y_{Bi}, z_{Bi}).

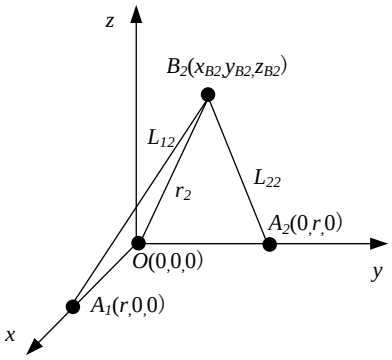

Fig. 5. Relative position of the measurement reference point to the point to be measured.

Using the coordinates of the three measurement reference points, and the distance between the three measurement reference points and the measured points on the docking surface of the moving components, we obtain the following equations:

$$x_{Bi}{}^2 + y_{Bi}{}^2 + z_{Bi}{}^2 = r_i^2 \tag{2}$$

$$(x_{Bi} - r)^2 + y_{Bi}{}^2 + z_{Bi}{}^2 = L_{1i}{}^2 \tag{3}$$

$$x_{Bi}{}^2 + (y_{Bi} - r)^2 + z_{Bi}{}^2 = L_{2i}{}^2 \tag{4}$$

where i = 1,2,3.

Solving equations (2)-(4) yields:

$$x_{Bi} = \frac{r^2 + r_i{}^2 - L_{1i}{}^2}{2r}$$

$$y_{Bi} = \frac{r^2 + r_i{}^2 - L_{2i}{}^2}{2r}$$

$$z_{Bi} = \sqrt{r_i{}^2 - x_{Bi}{}^2 - y_{Bi}{}^2}$$

where i = 1,2,3.

By equations (2) to (4), three spheres intersect at two points. It is evident that the plane mentioned here should be $z = 0$. According to Fig. 4 and Fig. 5, the point of interest has the positive z coordinate, $z_{Bi} > 0$, which leads to the solution for z_{Bi}.

D. The solution to the pose deviation

The calculation of the relative pose of the two components is equivalent to the calculation of the conversion relationship between the coordinate systems of the two components. The conversion relationship between the two coordinate systems can be expressed by seven parameters: three rotation parameters, three translation parameters, and one scale parameter. In other words: if we have the coordinates of the three points in the fixed coordinate system and then obtain the coordinates of the three points in the moving coordinate system with respect to the moving coordinate system and fixed coordinate system, the coordinate conversion relationship between the two coordinate systems can be solved. Since the scaling of the two coordinate systems {A} and {B} is the same in all directions and the coordinates of the three points B1, B2 and B3 in the two coordinate systems {A} and {B} are known, these seven parameters can be uniquely determined.

The scale parameter in this model is 1, so the transformation model between the two coordinate systems can be expressed as:

$$\begin{bmatrix} x \\ y \\ z \end{bmatrix}_A = \begin{bmatrix} \Delta x \\ \Delta y \\ \Delta z \end{bmatrix} + R \begin{bmatrix} x' \\ y' \\ z' \end{bmatrix}_B \tag{5}$$

where R is the rotation matrix, Δ is the translation vector, and A, B are the coordinates in the {A} and {B} coordinate system, respectively.

The rotation matrix R is a 3x3 orthogonal matrix with 3 degrees of freedom and can be constructed using the antisymmetric matrix S:

$$S = \begin{bmatrix} 0 & -c & -b \\ c & 0 & -a \\ b & a & 0 \end{bmatrix}$$

Using the antisymmetric matrix S to construct the rotation matrix R in the process of calculation [20]-[22] simplifies the analytical calculation process. This is not limited to the single model described above, but the calculation process remains unchanged even if the position of the measurement points on the movable component varies.

So

$$R = (I - S)^{-1} \cdot (I + S) \tag{6}$$

where I is the identity matrix. The rotation matrix R has only three variables a, b and c, and by solving for these three variables, R can be obtained.

On substituting points B_1 and B_2 into (5) and subtracting the two resulting equations to eliminate Δx, Δy and Δz, we obtain the following equation:

$$\begin{bmatrix} B_{1Ax} - B_{2Ax} \\ B_{1Ay} - B_{2Ay} \\ B_{1Az} - B_{2Az} \end{bmatrix} = R \begin{bmatrix} B_{1Bx'} - B_{2Bx'} \\ B_{1By'} - B_{2By'} \\ B_{1Bz'} - B_{2Bz'} \end{bmatrix} \tag{7}$$

where B_{1AX} is the value of the x-axis coordinate of the point B_1 in the {A} coordinate system, which is a known quantity and can be simplified here by setting:

$$X_{A12} = B_{1Ax} - B_{2Ax}$$

Substituting the above equation into (7), we have:

$$\begin{bmatrix} X_{A12} \\ Y_{A12} \\ Z_{A12} \end{bmatrix} = R \begin{bmatrix} X_{B12} \\ Y_{B12} \\ Z_{B12} \end{bmatrix} \tag{8}$$

Substituting (6) into (8) gives:

$$(I - S) \begin{bmatrix} X_{A12} \\ Y_{A12} \\ Z_{A12} \end{bmatrix} = (I + S) \begin{bmatrix} X_{B12} \\ Y_{B12} \\ Z_{B12} \end{bmatrix}$$

Using the antisymmetric matrix S in the above equation, we obtain:

$$\begin{bmatrix} 1 & c & b \\ -c & 1 & a \\ -b & -a & 1 \end{bmatrix} \begin{bmatrix} X_{A12} \\ Y_{A12} \\ Z_{A12} \end{bmatrix} = \begin{bmatrix} 1 & -c & -b \\ c & 1 & -a \\ b & a & 1 \end{bmatrix} \begin{bmatrix} X_{B12} \\ Y_{B12} \\ Z_{B12} \end{bmatrix}$$

Expanding the above equation yields:

$$\begin{bmatrix} X_{A12} + cY_{A12} + bZ_{A12} \\ -cX_{A12} + Y_{A12} + aZ_{A12} \\ -bX_{A12} - aY_{A12} + Z_{A12} \end{bmatrix} = \begin{bmatrix} X_{B12} - cY_{B12} - bZ_{B12} \\ cX_{B12} + Y_{B12} - aZ_{B12} \\ bX_{B12} + aY_{B12} + Z_{B12} \end{bmatrix}$$

The above equation can be written in the form:

$$\begin{bmatrix} X_{A12} - X_{B12} \\ Y_{A12} - Y_{B12} \\ Z_{A12} - Z_{B12} \end{bmatrix} = \begin{bmatrix} -c(Y_{B12} + Y_{A12}) - b(Z_{B12} + bZ_{A12}) \\ c(X_{B12} + X_{A12}) - a(Z_{B12} + Z_{A12}) \\ b(X_{B12} + X_{A12}) + a(Y_{B12} + Y_{A12}) \end{bmatrix} \tag{9}$$

Since there are only two independent equations in (9), it is not possible to solve for the three unknown quantities a, b and c. If you substitute points B_1 and B_3 into the above model, a set of equations similar to equation (9) can be obtained. Combining the two sets of equations, we obtain three independent equations as follows:

$$\begin{bmatrix} X_{A12} - X_{B12} \\ Y_{A12} - Y_{B12} \\ Z_{A13} - Z_{B13} \end{bmatrix} = \begin{bmatrix} -b(Z_{B12} + Z_{A12}) - c(Y_{B12} + Y_{A12}) \\ -a(Z_{B12} + Z_{A12}) + c(X_{B12} + X_{A12}) \\ a(Y_{B13} + Y_{A13}) + b(X_{B13} + X_{A13}) \end{bmatrix} =$$

$$\begin{bmatrix} 0 & -b(Z_{B12} + Z_{A12}) & -c(Y_{B12} + Y_{A12}) \\ -a(Z_{B12} + Z_{A12}) & 0 & c(X_{B12} + X_{A12}) \\ a(Y_{B13} + Y_{A13}) & b(X_{B13} + X_{A13}) & 0 \end{bmatrix} \begin{bmatrix} a \\ b \\ c \end{bmatrix}$$

We can now derive the solution to the above equation,

$$\begin{bmatrix} a \\ b \\ c \end{bmatrix} = \begin{bmatrix} 0 & -(Z_{B12} + Z_{A12}) & -(Y_{B12} + Y_{A12}) \\ -(Z_{B12} + Z_{A12}) & 0 & (X_{B12} + X_{A12}) \\ (Y_{B13} + Y_{A13}) & (X_{B13} + X_{A13}) & 0 \end{bmatrix}^{-1} \begin{bmatrix} X_{A12} - X_{B12} \\ Y_{A12} - Y_{B12} \\ Z_{A13} - Z_{B13} \end{bmatrix}$$

Substituting *a*, *b* and *c* into (6), the rotation matrix R can be determined.

The fixed X-Y-Z Euler angles are used to represent the three rotational degrees of freedom of the component in space. α, β, and γ represent the rotation angles around the *x*-axis, *y*-axis and *z*-axis, respectively. When $\sin\alpha = s\alpha$, $\cos\alpha = c\alpha$, β and γ are identical, the rotation matrix *R* can be expressed as:

$$R_{(\alpha,\beta,\gamma)} = \begin{bmatrix} c\beta c\gamma & s\alpha s\beta c\gamma - c\alpha s\gamma & c\,\alpha\, s\,\beta\, c\,\gamma + s\alpha s\gamma \\ c\beta s\gamma & s\alpha s\beta s\gamma + c\alpha c\gamma & c\alpha s\beta s\gamma - s\alpha c\gamma \\ -s\beta & s\alpha c\beta & c\alpha c\beta \end{bmatrix}$$

Considering the first column of the matrix, the sum of the squares of elements r_{11} and r_{21} is $c^2\beta$ ($c^2\gamma + s^2\gamma$) = $c^2\beta$, then β can be determined by $\sqrt{{r_{11}}^2 + {r_{21}}^2}$ and r_{31}. In addition, γ can be calculated from r_{11} and r_{21}, and α can be calculated from r_{32} and r_{33}. Assuming $c\beta \neq 0$, the following equation is obtained:

$$\beta = A\,tan\,2\left(-r_{31}, \pm\sqrt{{r_{11}}^2 + {r_{21}}^2}\right)$$

$$\gamma = A\,tan\,2\,(r_{21}/c\beta, r_{11}/c\beta)$$

$$\alpha = A\,tan\,2\,(r_{32}/c\beta, r_{33}/c\beta)$$

where *A tan 2* (*y*, *x*) is a four-quadrant arctangent function. The quadrant of the angle is determined based on the signs of *x* and *y*, and the angle value is then obtained by calculating *arctan* (*y*/*x*).

Finally, substituting the coordinates of any point from B_1, B_2, or B_3 in coordinate systems {A} and {B} into (5), we obtain the three translation degrees of freedom Δx, Δy and Δz for the component in space.

4. MEASUREMENT UNCERTAINTY ANALYSIS AND SIMULATION

We assume that the radius *r* of the circular dimension is 3.9625 m for the moving and fixed components. The distance between the measuring points can be measured and the length of the connecting lines between the measuring points is given in Table 1.

Based on the above known radius of the circular component and the length of the line between the measurement points, the relative displacement and the rotation angle of the two components can be solved in six degrees of freedom.

Table 1. The length of the connecting line between the measuring points.

r_1	r_2	r_3
6.2183	10.7365	9.4236
L_{11}	L_{12}	L_{13}
6.8893	11.3564	10.1536
L_{21}	L_{22}	L_{23}
8.5197	8.9258	11.8743

The relative displacements Δx, Δy and Δz of the two components in the three translational degrees of freedom in space are 3.6169 m, -3.8736 m, and 6.2632 m, respectively.

The relative rotation angles α, β and γ of the two components in the three rotational degrees of freedom in space are -102.5053°, -58.5727°, and 24.2072°, respectively.

Assuming that the measurement standard uncertainties of the direct measurements of each sensor are equal to U_L, let

$L_i = r_1, r_2, r_3, L_{11}, L_{12}, L_{13}, L_{21}, L_{22}, L_{23}$ (I = 1-9),

the six degrees of freedom functions

f_j ($L_1, L_2, L_3, L_4, L_5, L_6, L_7, L_8, L_9$), ($j$ = 1-6)

are determined by the nine variables L_i, and the standard uncertainty components of the six degrees of freedom being measured caused by L_i are:

$$U_i = |\frac{\partial f}{\partial L_i}|U_L \tag{10}$$

Since the measurement standard uncertainties of the direct measurements of the individual sensors are independent of each other, the synthetic standard uncertainty U_C can be expressed as:

$$U_C = \sqrt{\sum_{i=1}^{9} {U_i}^2} \tag{11}$$

Substitute the data in Table 1 into (10) and (11) to obtain the relational equation for the synthetic standard uncertainty caused by the standard measurement uncertainty U_L of the direct measurements of each sensor in determining the relative displacements of the moving and fixed components in six degrees of freedom. The relationship for the synthetic standard uncertainty caused by the standard measurement uncertainty U_L of the direct measurements of each sensor in the six degrees of freedom is given in Table 2.

Table 2. Synthetic standard uncertainty relationship equation on six degrees of freedom

Six degrees of freedom orientation	Synthetic standard uncertainty relationship equation
Translation along *x*-axis	$U_{ct}1 = 4.4350 * U_L$
Translation along *y*-axis	$U_{ct}2 = 3.3401 * U_L$
Translation along *z*-axis	$U_{ct}3 = 4.1332 * U_L$
Rotation around *x*-axis	$U_{calpha} = 0.7142 * U_L$
Rotation around *y*-axis	$U_{cbeta} = 1.4669 * U_L$
Rotation around *z*-axis	$U_{cgamma} = 2.5456 * U_L$

Using the synthetic standard uncertainty U_C as the measurement uncertainty for the estimated value *y* of the spatial six degrees of freedom offset *Y*, the offset of the component in the spatial six degrees of freedom can be expressed as:

$$Y = y \pm U_C$$

Analysis of Table 2 shows that the synthetic standard uncertainty is most affected in the *x*-axis translation direction and least affected in the *x*-axis rotation direction. In practical testing, it is also essential to comprehensively analyze the various factors that affect the test results and consider all sources of uncertainty in the test results.

5. CONCLUSIONS

In this paper, a method for determining the docking pose of large components based on the draw-wire displacement sensor was proposed and a corresponding measurement system was established; a mathematical model of the draw-wire measurement system was proposed and the application of the three-sphere rendezvous positioning principle was optimized in it; the relative pose relationship between the fixed and moving coordinate systems was solved under this model. An analysis and simulation of the measurement uncertainty of the relative pose relationships under the model was performed. The relative displacement and rotation angle of the two components in the six degrees of freedom, as well as the synthetic standard uncertainty caused by the standard measurement uncertainty of each sensor were obtained. The analysis results showed that the standard synthetic uncertainty is most affected in the x-axis translation direction and least affected in the x-axis rotation direction.

Unlike commonly used devices, such as laser trackers, which required the establishment of ground reference points to determine specific vector orientations, this method required only a few scalar data points, namely the distance between the corresponding point on the moving and fixed components, to correctly adjust the pose of the components during the assembly process. This method used a draw-wire displacement sensor that can detect the distance between two components at multiple points without interruption. Compared with existing measurement methods using optics and images, this method can avoid light obscuration, improve the accuracy of attitude measurement, reduce assembly cost, reduce manual labor, and improve assembly efficiency.

ACKNOWLEDGMENT

This work was supported by the Department of Science and Technology of Shaanxi Province, China (grant # 2020ZDLGY14-02, grant # 2019zdzx01-02-02).

REFERENCES

[1] Naing, S. (2004). *Feature based design for jigless assembly*. PhD Thesis, Cranfield University, Cranfield, UK.

[2] Mei, B., Zhu, W. (2021). Accurate positioning of a drilling and riveting cell for aircraft assembly. *Robotics and Computer-Integrated Manufacturing*, 69, 102112. https://doi.org/10.1016/j.rcim.2020.102112

[3] Yang, B., Yu, C., Jin, Z., Li, J., Li, M. (2015). Thermal deformation error modeling and compensation approach for laser tracker orientation. *Acta Aeronauticaet Astronautica Sinica*, 36 (9), 3155-3164. https://doi.org/10.7527/S1000-6893.2014.0217

[4] Jin, Z.-J., Li, J.-X., Yu, C.-J., Ke, Y.-L. (2015). Registration error analysis and evaluation in large-volume metrology system. *Zhejiang Daxue Xuebao (Gongxue Ban) / Journal of Zhejiang University (Engineering Science)*, 49 (4), 655-661.

[5] Han, L., Mi, L., Liu, X., Teng, Q., Tang, Q., Xia, Y. (2021). Measurement method of geometric error of coordinate measuring machine using laser tracer. *Advanced Engineering Sciences*, 53 (3), 159-165.

[6] Wang, W., Yu, Z., Guo, Y., Yang, X. (2014). Study on the occlusion problem in dynamic space intersection measurement with multi-camera systems. *Acta Optica Sinica*, 34 (4), 415003. http://dx.doi.org/10.3788/aos201434.0415003

[7] Chen, Y., Zhou, F., Zhou, M., Zhang, W., Li, X. (2020). Pose measurement approach based on two-stage binocular vision for docking large components. *Measurement Science and Technology*, 31, 125002. http://dx.doi.org/10.1088/1361-6501/aba5c7

[8] Choi, A.J., Park, J., Han, J. H. (2022). Automated aerial docking system using onboard vision-based deep learning. *Journal of Aerospace Information Systems*, 19 (6), 421-436. https://doi.org/10.2514/1.I011053

[9] Ceccarelli, M., Carrasco, C. A., Ottaviano, E. (2000). Error analysis and experimental tests of CATRASYS (Cassino Tracking System). In *2000 26th Annual Conference of the IEEE Industrial Electronics Society. IECON 2000. 2000 IEEE International Conference on Industrial Electronics, Control and Instrumentation*. IEEE, 2371-2376. https://doi.org/10.1109/IECON.2000.972368

[10] Luo, Z., Sun, S., Mei, J., Chen, L., Xu, J. (2017). Application research of robot calibration based on draw-wire displacement sensors. *Aeronautical Manufacturing Technology*, 9, 43-49. http://www.amte.net.cn/CN/10.16080/j.issn1671-833x.2017.09.043

[11] Jiao, X., Zheng, G., Jia, X. (2020). Based on cable displacement sensors dynamic displacement measurement in space. *Chinese Journal of Electron Devices*, 3, 619-623.

[12] Wang, G., Wang, W., Wang, C. (2017). The method and error analysis of deep-sea pose measurement system. *Measurement*, 98, 276-282. https://doi.org/10.1016/j.measurement.2016.11.002

[13] Zhang, B., Liu, H., Wang, T., Wang, Z., Ma, H. (2022). Research and experiment of rope measurement method for subsea pipeline based on uncertainty analysis. *Measurement*, 201, 111698. https://doi.org/10.1016/j.measurement.2022.111698

[14] Arun, K. S., Huang, T. S., Blostein, S. D. (1987). Least-squares fitting of two 3-D point sets. *IEEE Transactions on Pattern Analysis and Machine Intelligence*, PAMI-9 (5), 698-700. https://doi.org/10.1109/TPAMI.1987.4767965

[15] Wang, Z., Jepson. (1994). A new closed-form solution for absolute orientation. In *1994 Proceedings of IEEE Conference on Computer Vision and Pattern Recognition*. IEEE, 129-134. https://doi.org/10.1109/CVPR.1994.323819

[16] Hill, A., Cootes, T. F., Taylor, C. J. (1996). Least-squares solution of absolute orientation with non-scalar weights. In *Proceedings of 13th International Conference on Pattern Recognition*. IEEE, 461-465. https://doi.org/10.1109/ICPR.1996.546069

[17] Cheng, S., Wu, H., Yao, Y., Liu, F., Miao, Q., Li, C., Zhu, J. (2010). An analytical method for the forward kinematics analysis of 6-SPS parallel mechanisms. *Journal of Mechanical Engineering*, 46 (9), 26-31.

[18] He, X., Shi, Z., Zeng, D., Lei, P., Liu, C. (2019). Posture calculating algorithm based on LM algorithm for large part docking. *Aeronautical Manufacturing Technology*, 62 (8), 44-48. http://www.amte.net.cn/CN/10.16080/j.issn1671%E2%80%93833x.2019.08.044

[19] Wang, Z., Cheng, S., Liu, C., Wang, J. (2016). Three-dimensional weighted centroid indoor positioning algorithm based on sphere intersection. *Journal of China University of Mining & Technology*, 45 (5), 944-950.

[20] Hamano, F. (2013). Derivative of rotation matrix direct matrix derivation of well known formula. In *arXiv*:1311.6010. https://doi.org/10.48550/arXiv.1311.6010

[21] Liang, K. K. (2018). Efficient conversion from rotating matrix to rotation axis and angle by extending Rodrigues' formula. In *arXiv*:1810.02999. https://doi.org/10.48550/arXiv.1810.02999

[22] Zhu, C., Jun, L., Huang, B., Su, Y., Zheng, Y. (2022). Trajectory tracking control for autonomous underwater vehicle based on rotation matrix attitude representation. *Ocean Engineering*, 252, 111206. https://doi.org/10.1016/j.oceaneng.2022.111206

Received June 21, 2023
Accepted September 25, 2023